

Effect of Isolated Nickel Tolerant Bacteria On Anatomical and Proteomic Responses in Nickel Tolerant Chickpea Cultivar

K Jyothsna^{1*} and B Sujatha²

^{1*}Research Scholar, Department Of Botany, Andhra University

²Professor, Department Of Botany, Andhra University, Visakhapatnam

*Corresponding Author: jyothsna@live.com

Received: 16th Dec, 2025; Revised: 8th Feb 2026; Accepted: 12th Feb, 2026; Available Online: 28th Feb, 2026

ABSTRACT

Nickel, an essential micronutrient is required to plants in low concentration. Agricultural soils contaminated by Ni, adversely effect plant growth. Excess concentration of Ni is toxic to plants causing anatomical damage, oxidative stress, disrupts cellular homeostasis and causes molecular alterations. The present study evaluates the effects of Ni stress on plants and plant growth promoting rhizobacteria MGNJ-01 that mitigates Ni toxicity in Ni tolerant chickpea cultivar *Cicer arietinum* (L.), ICCV 10102. This has been achieved by studying the anatomical, proteomic and *in silico* approaches. Ni toxicity or stress has caused marked reduction in root vascular tissue diameter and altered stomatal morphology, which has hampered the transport and gaseous exchange. Inoculation of PGPR MGNJ-01 to the chickpea plant under Ni toxicity significantly elevated root and leaf anatomical features. Proteomic analysis identified two differentially expressed key proteins Mn-SOD (Manganese superoxide dismutase) and LEA (Late embryogenesis abundant protein). Mn-SOD was observed under Ni stress and was responsible for antioxidative defense, while LEA was prominent under Ni + PGPR treated condition indicating improved cellular protection. *In silico* characterisation and protein-protein interactions confirmed the functional stability and central roles in stress tolerance. These observations highlight that, PGPR is a sustainable strategy to alleviate Ni stress in Ni tolerant chickpea cultivar ICCV 10102.

Keywords: Nickel stress, Chickpea, PGPR, Proteomics, Mn-SOD, LEA, Protein-Protein interaction

How to cite this article: Jyothsna K, Sujatha B, Effect of Isolated Nickel Tolerant Bacteria On Anatomical and Proteomic Responses in Nickel Tolerant Chickpea Cultivar. *Int J Drug Deliv Technol.* 2026;16(9s): 900-911. DOI: 10.25258/ijddt.16.9s.94

Source of support: Nil.

Conflict of interest: None

INTRODUCTION

Contamination of agricultural soils by heavy metals is emerging as a major environmental hazard, limiting crop production and food security. Nickel (Ni) an essential micronutrient for plants at low concentrations, is considered as a heavy metal. Accumulation of Ni in soil leads to severe toxic effects on plants that include impaired growth, altered metabolism, oxidative stress, disruption of cellular and anatomical structures *Cicer arietinum*, commonly known as chickpea plays a vital role in human nutrition and soil fertility through biological nitrogen fixation. This plant is vulnerable to heavy metal stress making its yield a concern in its production. Plants exposed to Ni stress exhibit a cascade of events. Apart from root and leaf anatomy and changes in protein expression profiles, Ni induces generation of reactive oxygen species at cellular level leading to oxidative damage of membranes, proteins and nucleic acids. To withstand these adverse effects, plants activate complex defense mechanisms which involve antioxidant enzymes, stress responsive proteins and structural adaptations. Of late, use of plant growth promoting rhizobacteria (PGPR) is being considered as eco-friendly, economical and sustainable approach to mitigate heavy metal toxicity in plants. Under stress conditions, PGPR enhance plant growth by modulating the phyto-hormone levels, improving nutrient uptake, immobilising heavy metals and activating antioxidant defense systems. It was observed that bacterial inoculation has shown to alleviate metal induced stress by regulating physiological and molecular responses of plants due to which the stress tolerance and overall plant performance is improved. Stress induced molecular changes can be deciphered, by identifying the differentially expressed proteins that are involved in detoxification, antioxidative defense, cellular protection and metabolic regulation. To serve this purpose, proteomic analysis is of great use. Furthermore, *in silico* characterization and protein protein interaction (PPI) network analysis also provides valuable insights into the structural, functional and interactive properties of stress-responsive proteins which enables a deeper understanding.

The present study analyses, the effect of Ni stress and Ni stress coupled with PGPR inoculation on a Ni tolerant chickpea cultivar ICCV 10102. This has been achieved by integrating anatomical, proteomic and bioinformatic approaches. This study is focused

on, i) evaluating Ni, Ni + Bacteria induced anatomical changes in roots and leaves against control. ii) Identified the differentially expressed proteins under Ni stress and Ni + Bacterial inoculation using SDS-PAGE and MALD-TOF/MS and iii) Performed *in silico* characterisation and PPI network analysis of stress responsive proteins. This integrated approach provides comprehensive approach of beneficial PGPR mitigating Ni toxicity and enhancing stress tolerance in chickpea.

1. Material Methods:

A Nickel tolerant chickpea cultivar (ICCV 10102) was chosen and was examined for the possible effects under exclusive Nickel stress, bacterial inoculation and nickel stress with bacterial inoculation against control. Anatomical changes in root and leaf were observed along with proteomic responses in the leaf. The experiment was conducted under four groups as control, Ni treated, Bacterial cells treated and Ni + Bacteria treated. The seedlings in all the four experimental groups were treated every alternate day with respective solutions and bacterial inoculum for 3 weeks.

1.1. Anatomy

Anatomical changes in root and leaf from all the experimental groups were performed by observing under the microscope. Root and first fully expanded leaves from all the experimental groups were fixed in FAA (16) for 72 hours and then kept in 70% ethyl alcohol. The upper and lower epidermis is peeled and stained by safranin (21). Cross sections of root were stained with 1% safranin and 50% glycerin was used for mounting. The slides were examined and photographed using a Lynx light microscope and captured by capture 2.4 HDMI camera.

2. Identification and Characterisation of differential proteins under Ni-stress in ICCV 10102 with bioinoculant.

2.1 Protein Extraction

0.5gm of fresh and young leaves of each experimental groups were homogenised separately with 2ml extraction buffer containing 50mM Tris-Glycine (pH 8.3), 0.5M Sucrose, 50mM EDTA, 0.1M KCl, 2mM PMSF and 0.1% 2-mercapto ethanol in chilled mortar and pestle. The homogenate was centrifuged at 14000rpm for 10 minutes at 4°C. The supernatants were stored at -20°C for further analysis.

*Author for Correspondence: jyothsna@live.com

2.2. Protein separation by SDS-PAGE & Peptide elution from gel

To separate the proteins by SDS-PAGE, 0.1ml of extracted protein samples from all the experimental groups were suspended in sample loading buffer added in a ratio of 3:1 of sample volume to sample buffer. The sample loading buffer consists of 0.5M Tris-HCl (pH 6.8), 20.2% (v/v), glycerol 0.0001% (w/v) SDS, 0.03% 9w/v) Dithiothreitol (DTT) and 0.04% (v/v) 2-mercaptoethanol. The protein and the sample loading buffer were boiled at 95°C for 5min and kept in ice before loading into the gel. 12% resolving gel was prepared by 1.5M Tris-HCl (pH 8.8), 20% SDS, 10% ammonium persulphate and TEMED. 0.5M Tris-HCl (pH6.8), 20% SDS, 10% ammonium persulphate and TEMED were used to prepare 5% stacking gel. Electrophoresis was accomplished at 100V for 1hr using Vertical Electrophoretic unit with running buffer that consisted 25mM tris base, 192mM glycine and 3mM SDS. The gel was stained with 0.5% Coomassie Brilliant Blue R-250 in 45% (v/v) methanol, 10% (v/v) acetic acid for 1hr and destained for 12hrs in 20% (v/v) methanol and 10% (v/v) acetic acid. The gel was washed with distill water until a clear background, before being viewed and photographed with Geldoc. The differentially expressed peptide bands were extracted from the gel, cut into smaller fragments and squashed carefully. They were then washed twice with 50% acetonitrile in 25mM ammonium bicarbonate for 15 minutes at room temperature, immersed and homogenised in elution buffer. The homogenate was centrifuged at 10000rpm for 10minutes at -4°C.

2.3. Identification of Peptide

The extracted peptide bands were identified by protein mass finger printing (PMF) using MALDI-TOF/MS (Applied Biosystems, Foster city, CA). The eluted protein fractions were subjected to trypsin digestion (1mg/ml) at 37°C for overnight. 0.5µL of digested peptide sample is injected onto a matrix that comprised saturated α-cyano-4-hydroxycinnamic acid prepared in 50% acetonitrile and 5% trifluoroacetic acid. Data from the mass spectrometer is obtained in reflector mode in the mass range of 700-5000 Da. The raw data from the mass spectrometer is processed by GPS Explorer software and generated a peak was generated using various settings such as, signal-to-noise filtering, an exclusion list and depositing factors. The generated mass spectrum is subjected to homology searching against sequence databases using MASCOT software. The score acquired from MASCOT software analysis is crucial to showing the likelihood of a genuine positive identification and had to be at least 50.

2.4. In silico characterisation of identified proteins.

The amino acid sequence of identified proteins was retrieved from NCBI and the sequences were subjected to further analysis in FASTA format.

ExPasy's ProtParam server was used to compute the physicochemical properties. The secondary structural elements in the identified peptide were predicted by SOPMA (Self Optimized Prediction Method). The SOPMA algorithm initially explores the SWISSPORT database and identifies the most similar sequences by employing the FASTA programme. Subsequently, by using the CLUSTAL programme, the query sequence is aligned with the list of identified homologous protein sequences and finally SOPMA was applied to each aligned sequence to predict the ability of amino acids to exhibit different secondary structural elements including alpha helices, β sheets, random coils and loops. To predict the 3D structure of identified proteins, *ab initio* method alongside the swiss model (18) were used. PROCHECK server was used to validate the predicted 3D model of identified proteins by Ramachandran plot analysis. Additionally, the accuracy of predicted 3D structure was validated using ERRAT. The protein-protein interactions were studied by using STRING analysis

(7). The PPI network was constructed by using PPI couples that had protein interaction values greater than 0.4. An analysis of topological features of PPI networks including betweenness and node degree, was conducted using the Centiscape v2.1 plug-in in the Cytoscape Desktop v 3.4.0 (6)

3. RESULTS AND DISCUSSION

3.1. Anatomy

The cross section of roots from all treatment groups displayed considerable heterogeneity in the diameter of vascular tissue. Under controlled and bacterial inoculation (MGNJ-01) conditions, the root displayed conventional anatomical features including a distinct epidermis, cortex, endodermis, pericycle and centrally positioned vascular structures. Exposure to 100µM Ni induced significant anatomical changes characterized by a considerable increase in thickness of epidermis and cortex. Xylem exhibited greater robustness, preserving the overall structural integrity of the root. The intercellular gaps in the cortex were restricted, signifying maintained cellular organisation. The control plants exhibited vascular tissue with a larger diameter, while Ni treated plants displayed a reduced diameter of vascular tissue. The diameters of vascular tissue from the roots of control, Ni-treated, MGNJ-01 treated and Ni + MGNJ-01 treated groups were measured as 255.727, 122.898, 319.829 and 203.828µm respectively.

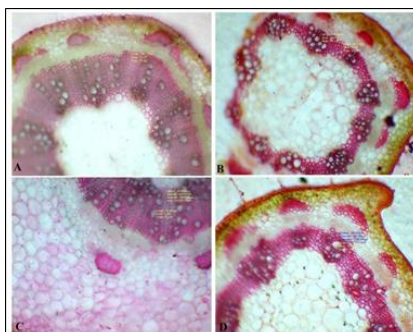


Fig 1: Root cross-sections A) Control B) Ni-treated C) MGNJ-01-treated D) Ni + MGNJ-01 treated.

Microscopic analysis of leaf stomata demonstrated significant morphological variations across all treatment groups are displayed in table 1.

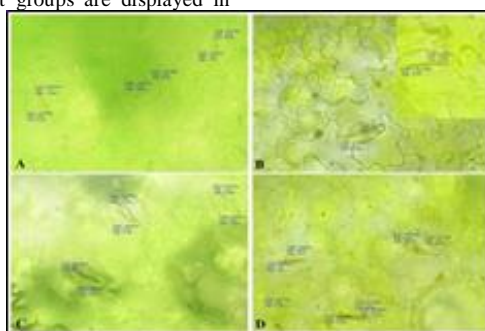


Fig 2: Micrographs of stomatal anatomy A) Control B) Ni-treated C) MGNJ-01 treated

D) Ni + MGNJ-01 treated.

Table 1. Stomatal dimensions from all the treatment groups of chickpea cultivar

S. No.	Treatment Group	Stomatal dimensions (µm)	
		Length	Width
1	Control	235.606	192.892
2	Ni treated	242.774	112.586
3	MGNJ-01 treated	280.820	171.492
4	Ni + MGNJ-01 treated	267.570	178.880

This study revealed that chickpea roots displayed notable structural changes due to Ni stress and showed beneficial effects of MGNJ 01 treatment. The results align with the findings of (30) and 1Ahmad *et al.*, (2015) who mentioned that the significant thickening of cell walls, especially in the endodermal region, potentially indicating suberization as a defensive mechanism to limit metal absorption. (40) found xylem vessels decreased in diameter and distorted which may impair water and nutrient uptake, transport and eventually affects plant growth. (23) reported that application of PGPR may improve antioxidant enzyme functioning, mitigate oxidative damage and promote healthy root development. This study revealed significant variations in stomatal features of chickpea leaves exposed to Ni stress and those inoculated with PGPR under Ni stress. Under controlled conditions, leaves displayed typical stomatal density, size and shape reflecting appropriate physiological performance. Under Ni stress, they exhibited diminished stomatal density, smaller malformed guard cells and an increased prevalence of partially closed or collapsed stomata. These findings align with earlier studies by (31) and 1Ahmad *et al.*, 2012) which indicated that heavy metal stress hinders stomatal growth and function, resulting in compromised gas exchange and diminished photosynthetic efficiency. (32) posited that, decrease in stomatal density and modified guard cell morphology under Ni stress may result from metal induced oxidative stress that disrupts cellular differentiation and diminished stomatal aperture and the prevalence of aberrant stomata indicating that Ni stress constrains transpiration and carbon dioxide assimilation, impairing plant development and productivity.

The current investigation demonstrated that MGNJ-01 treated plants under Ni stress had enhanced stomatal density, more uniform and turgid guard cells and a reduced incidence of aberrant stomata in comparison to plants exposed solely to Ni stress. These findings correspond to studies of (9) and (25) which indicated that PGPR inoculation augments plant tolerance to heavy metal stress by regulating phytohormone levels enhancing nutrient absorption and mitigating oxidative damage. (23) indicated that PGPR are recognised for enhancing stomatal growth and sustaining cellular homeostasis during stressful circumstances. The beneficial effects of PGPR may involve mechanisms like generation of ACC deaminase, siderophores and exopolysaccharides, which together immobilize metals, thereby safeguarding root tissues and enhancing leaf Architecture (10; 28).

3.2. Evaluation of Proteomic response

Protein bands were observed by SDS-PAGE analysis. Control, Ni-treated, MGNJ-01 treated and Ni + MGNJ-01 treated protein bands were compared across lanes with molecular weights determined using a protein marker (M) spanning from 11 kDa to 245 kDa. The current work demonstrated that majority of protein bands were analogous across all

four treatment groups. However, a significant alteration occurred under controlled and stressful situations. All lanes had unique protein bands signifying the existence of diverse protein species within each treatment. Prominent bands were seen at approximately 63, 48 and 35kDa in all samples indicating that these proteins are constitutively produced in chickpea irrespective of treatment.

Under Ni treatment, a significant emergence of novel band at around 25 kDa suggests that Ni stress specifically produces this protein. MGNJ-01 treatment group displayed an additional distinct peptide band at 15 kDa showing that bacterial treatment specifically induces this protein. Ni + MGNJ-01 treatment group displayed the presence of ~25 kDa peptide band which was more pronounced than that observed in MGNJ-01-treated group. These proteins are likely associated with the plant's response to simultaneous Ni stress and beneficial microbial interactions. The expression of 25 kDa and 15 kDa proteins in this work aligned with the findings of (39) which indicated that heavy metal stress including Ni exposure, causes significant physiological and biochemical alterations in plants, frequently leading to modified protein expression. Similarly, (33) indicated that heavy metal stress predominantly results in the modification of pre-existing proteins rather than the production of completely new proteins.

These differentially expressed proteins were associated with several cellular and physiological functions which include osmoregulation, photosynthesis, carbohydrate metabolism, redox homeostasis and ion balance. (20) asserted that alterations in a living environment or cellular function led to corresponding modifications in the cell's proteome to adapt to diverse conditions. (36) indicated that, treatment with PGPR alone did not give significant alterations in the protein profile relative to the control, implying that PGPR inoculation under non-stress conditions may not substantially modify the principal soluble proteins. Our findings align with those of (11) indicating that stress leads to an increased accumulation of proteins potentially responsible for the particular production of salt shock proteins with molecular weights of 15, 28 and 72 kDa in resistant genotypes.

The protein bands having molecular weight 25 kDa and 15 kDa were extracted from the gel and subjected to in-gel digestion and analysed by matrix assisted laser desorption ionisation-time of flight mass spectrometry (MALDI-TOF-MS). The obtained peptide mass fingerprints were used to search the National Centre for Biotechnology Information database using mascot. Peptide identification results of 25 and 15 kDa from Ni-treated and Ni + MGNJ-01 treated groups were illustrated in the table 2 and the figures (figures 3 and 4) for MALDI-TOF-MS spectra of 25 kDa and 15 kDa protein bands from Ni treated leaf and Ni + MGNJ-01 treated leaf are given below.

Table 2: Proteins identified from the 25 and 15 k Da SDS gel bands

Source Organism	Protein Band	Max. homology (protein name)	Best match organism	Expt/Theor. Mw (KD)	Score (MS/M S)	Acces. No.
<i>Cicer arietinum</i>	25 kDa	Mn-SOD	<i>Lathyrus oleraceus</i>	25/27	97%	P27084
<i>Cicer arietinum</i>	15 kDa	LEA	<i>Cicer arietinum</i>	14/13	94%	AI199863.1

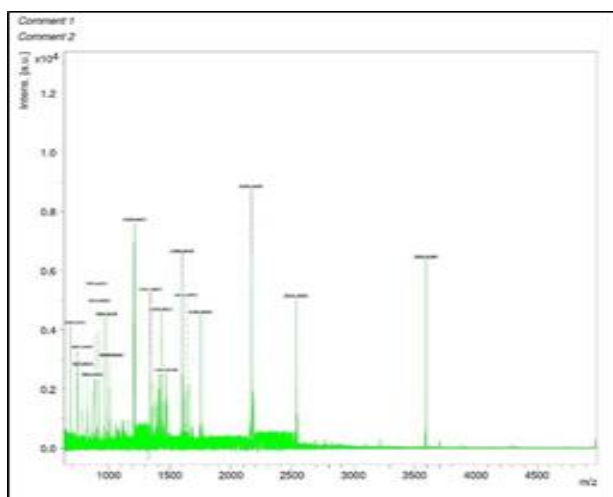


Fig 3: MALDI-TOF MS spectra of 25 kDa protein protein band from Ni treated leaf.

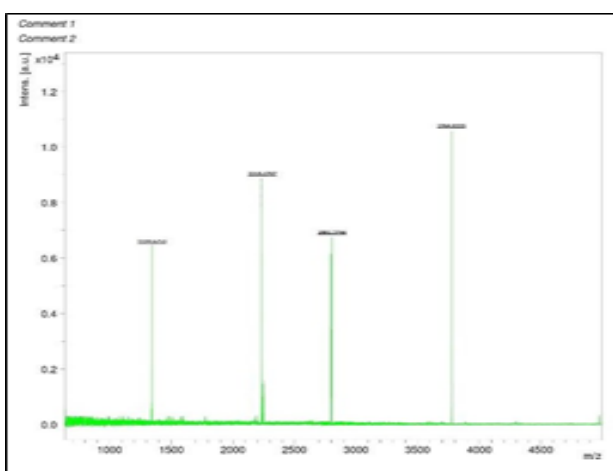


Fig 4: MALDI-TOF MS spectra of 15 kDa band from Ni + MGNJ-01 treated leaf

These results imply that chloroplast and mitochondria are the mostly influenced organelles inside the cells by heavy metals stress. Proteome analysis of chickpea leaf proteins suggest that a complex cellular network is influenced by Ni stress. MnSOD is an important antioxidant enzyme found mainly in mitochondria catalysing the dismutation of superoxide radicals into hydrogen peroxide and molecular oxygen, thereby protecting plant cells from oxidative damage caused by abiotic stresses including heavy metal toxicity (2). PMF analysis in the current study revealed the up-regulation of MnSOD in chickpea leaves subjected to Ni stress, indicating the generation of reactive oxygen species as a response to Ni toxicity. In agreement with the present findings, (32) showed that higher MnSOD levels in legumes indicate an active defense mechanism to attenuate oxidative damage generated by Ni. (13) asserted that PGPR can mitigate metal induced oxidative stress by augmenting antioxidant enzyme activities and improving overall plant viability.

PMF identification of LEA proteins in Ni + MGNJ-01 treated chickpea leaves highlight their potential function in cellular protection under stress

conditions. (17) asserted that PGPR are recognised for inducing systemic tolerance in host plants potentially by activating stress-responsive pathways, including those associated with LEA proteins. These are hydrophilic proteins most frequently connected with dehydration and osmotic stress tolerance, though they are being acknowledged for their role in regulating plant responsiveness to heavy metal stress (4). PMF based proteomic analysis indicate that both Mn-SOD and LEA proteins are key components of chickpea leaf proteome in response to Ni stress and its amelioration by PGPR. Their varied expression highlights the intricate network of antioxidative and protective mechanisms, employed by plants to mitigate heavy metal toxicity with beneficial microorganisms, further augmenting these protective responses.

3.3. In-silico characterisation of Identified Proteins.

Physicochemical characterisation and the amino acid sequence of the proteins Mn-SOD and LEA retrieved from PDB were shown in the tables 3 and 4.

Table 3: Physicochemical characteristics of Mn-SOD and LEA proteins

Parameter	Mn-SOD	LEA
Total no. of amino acids	226	118
Molecular weight	25153.68 Da	13158.25 Da
pI	7.86	8.17
Positively charged residues	24	13
Negatively charged residues	23	12
Extinction coefficient	46410 M ⁻¹ cm ⁻¹	8480 M ⁻¹ cm ⁻¹

Instability index		27.98	22.22
Aliphatic index		94.60	103.05
GRAVY		-0.306	0.097
Half-life	In mammalian reticulocytes	30 hours	30 hours
	In yeast	>20 hours	>20 hours
	In <i>E. coli</i>	>10 hours	>10 hours
Formula		C1137H1779N309O330S3	C598H941N167O162S3

Table 4: Amino acid sequence of Mn-SOD and LEA proteins

Amino acid	Mn-SOD		LEA	
	No. of Residues	% of Residues	No. of Residues	% of Residues
Ala (A)	23	10.2	6	5.1
Arg (R)	6	2.7	7	5.9
Asn (N)	11	4.9	3	2.5
Asp (D)	10	4.4	4	3.4
Cys (C)	1	0.4	0	0.0
Gln (Q)	10	4.4	2	1.7
Glu (E)	13	5.8	8	6.8
Gly (G)	15	6.6	11	9.3
His (H)	10	4.4	8	6.8
Ile (I)	15	6.6	4	3.4
Leu (L)	25	11.1	13	11.0
Lys (K)	18	8.0	6	5.1
Met (M)	2	0.9	3	2.5
Phe (F)	4	1.8	7	5.9
Pro (P)	9	4.0	4	3.4
Ser (S)	14	6.2	8	6.8
Thr (T)	13	5.8	4	3.4
Trp (W)	6	2.7	1	0.8
Tyr (Y)	9	4.0	2	1.7
Val (V)	12	5.3	17	14.4
Pyl (O)	0	0.0	0	0.0
Sec (U)	0	0.0	0	0.0

The protein's instability index offers insights about its stability when tested in a controlled laboratory setting. A protein with an instability index below 40 is considered stable whereas, a number above 40 indicates potential protein instability (12). (41) discovered that minor factors located at the N-terminus have an impact on the stability of a protein, thereby affecting its lifespan. (29) found that proteins with a half-life of fewer than 5 hours, had an instability index greater than 40; while proteins with a half-life of more than 16 hours had an instability index less than 40. The decreased thermal stability suggests a structure that is more pliable (15). The negative grand average of hydropathicity

signifies that proteins possess a polar hydrophilic nature, resulting in enhanced interaction between the protein and water (24). This data suggests that the presence of ionizable amino acids on the protein surface, which are accessible to water, is the primary factor that affects the isoelectric point of proteins and protein complexes.

3.4. Secondary Structure

The secondary structural elements of Mn-SOD and LEA were predicted using SOPMA and are represented in the table 5 while the secondary structural elements are displayed in the figures 5 and 6.

Table 5: Secondary structural elements of Mn-SOD and LEA proteins.

Structural elements	Mn-SOD		LEA	
	No. of Residues	% of Residues	No. of Residues	% of Residues
Alpha helix (Hh)	108	47.79%	24	20.34%
310 helix (Gg)	0	0.00%	0	0.00%
Pi helix (Ii)	0	0.00%	0	0.00%
Beta bridge (Bb)	0	0.00%	0	0.00%
Extended strand (Ee)	28	12.39%	50	42.37%
Beta turn (Tt)	6	2.65%	10	8.47%
Bend region (Ss)	0	0.00%	0	0.00%
Random coil (Cc)	84	37.17%	34	28.81%
Ambiguous states	0	0.00%	0	0.00%
Other states	0	0.00%	0	0.00%

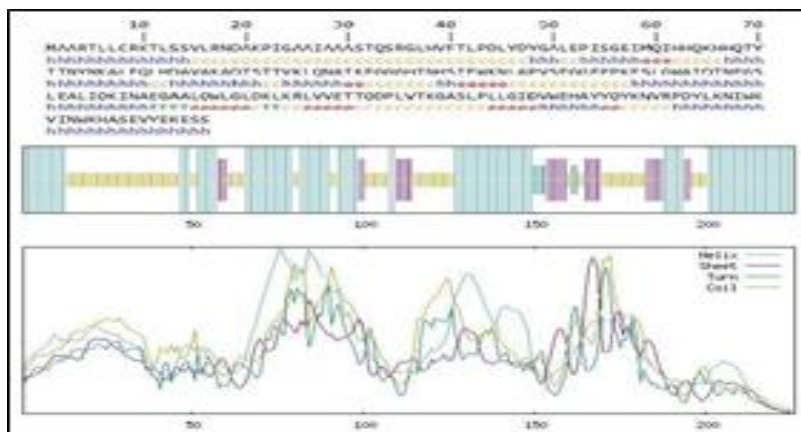


Fig 5: Secondary structural elements of Mn-SOD.

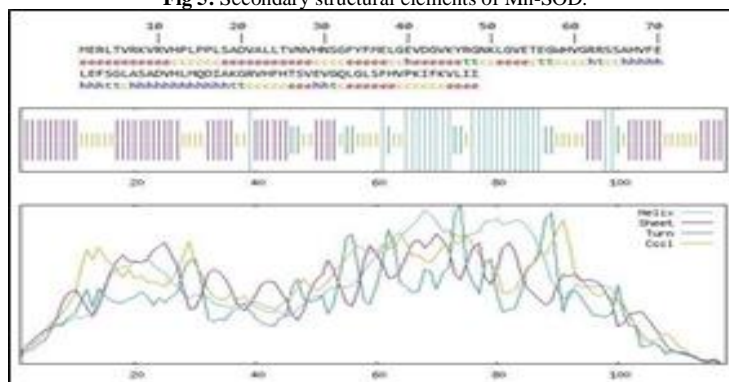


Fig 6: Secondary structural elements of LEA

Determining a protein's secondary structural configuration aids in comprehending the hydrogen bonds that exist within the protein, providing insights into its structural and functional efficacy (22). (5) stated that, random coils play crucial role in proteins by providing flexibility and facilitating conformational changes. The greater coil percentage is due to abundant proline residues. This possesses the distinctive characteristics of inducing bonds in polypeptide chains and disturbing organised secondary structure (37). (27) reported that the prevalence of the coiled sections suggest, a significant degree of preservation and robustness of protein structure. The presence of hydrophobic residues in a composition leads to favourable interactions with the hydrophobic lipid bilayer (35). (3) proposed that the structure of helical proteins determine their diverse functions which include signal recognition, receptor activity, transport of ions and molecules across

membranes, energy transfer and preservation.

3.5. 3D Structure

The 3D model of Mn-SOD peptide from Ni tolerant chickpea cultivar was predicted by employ protein ID IJYA9.1.A as a very suitable template, demonstrating a sequence homology of 87.17%, and complete coverage of 100%. The top ranked template in the PDB database is an alpha fold DB model of superoxide dismutase monomer in glycine max. 3D model of LEA peptide from Ni tolerant chickpea cultivar was predicted by employ protein ID A0A1S2 YM98.1.A. as a very suitable template, demonstrating a sequence homology of 98.29% and complete coverage of 100%. The top ranked template in the PDB database is an alpha fold DB model of uncharacterised protein monomer in *Cicer arietinum*. figures 7 and 8 show the predicted 3D models of Mn-SOD and LEA peptides.

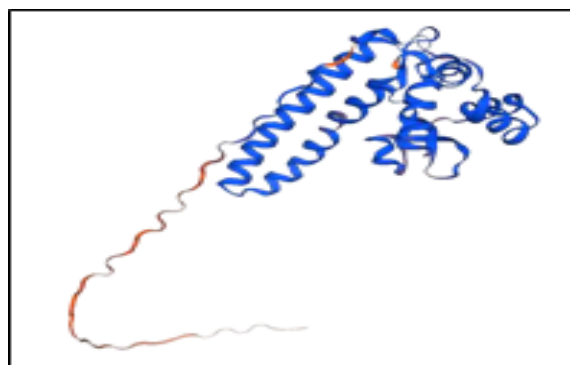


Fig 7: Predicted 3D of Mn-SOD

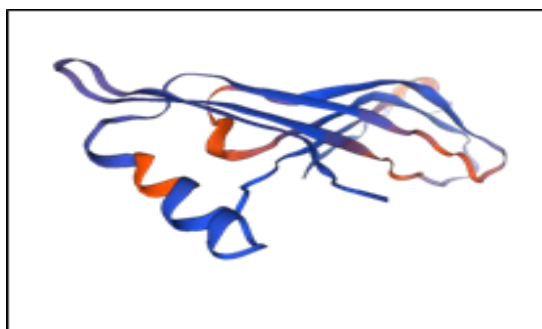


Fig 8: Predicted 3D of LEA

Quality assessment of predicted 3D model.

In the current investigation, the predicted 3D models of Mn-SOD and LEA peptides had QMEAN values of 0.87 and -0.77. The density map of QMEAN score demonstrates that the estimated reliability of these models

lie between 0 and 1. The QMEAN scores of the predicted models were almost zero suggesting a high quality model. Figures 9 and 10 demonstrated density graphs for the predicted models of Mn-SOD and LEA peptides.

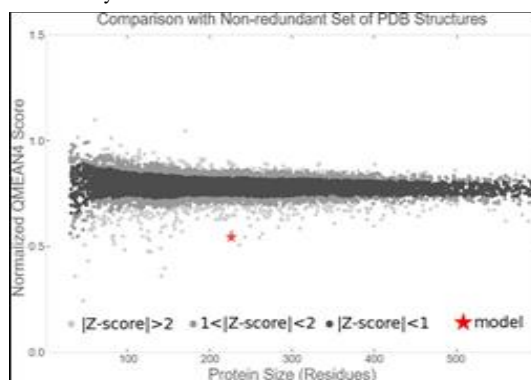


Fig 9: Plot showing QMEAN and Z-score of Mn-SOD.

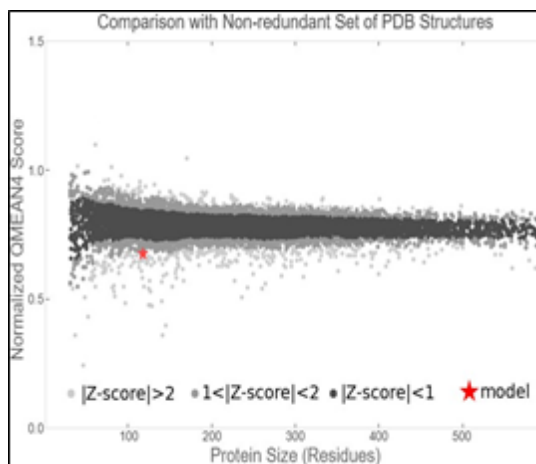


Fig 10: Plot showing QMEAN and Z-score of LEA

3.6. Model Validation

The structural validation of the predicted Mn-SOD and LEA models include analysing the geometrical features of the backbone confirmations which were performed using Ramachandran plot calculations with the

PROCHECK server. The statistics of the plots for Mn-SOD and LEA were presented in the table 6 while, Ramachndran Plots of Mn-SOD and LEA are depicted in figures 11 and 12.

Table 6: Ramachandran plot statistics of predicted Mn-SOD and LEA models

Residues	Mn-SOD		LEA	
	No. of Residues	% of Res idu es	N o. of Residues	% of Re sid ues
Most favoured regions	162	81	92	92
Additionally allowed regions	31	15.5	8	8
Generously allowed regions	3	1.5	0	0.0
Disallowed regions	4	2	0	0.0
Non-Glycine and Non-Proline	200	100	100	100
End Residues	2	-	2	-

Glycine	15	-	11	-
Proline	9	-	4	-

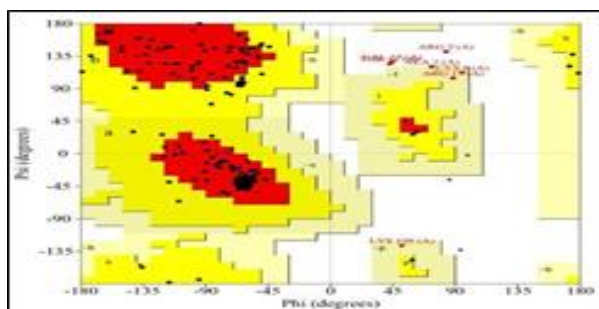


Fig 11: Ramachandran plot of Mn-SOD structural model predicted by PROCHECK

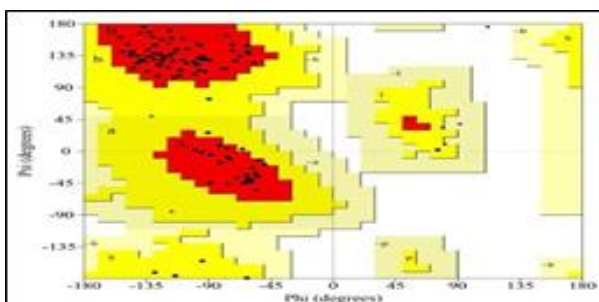


Fig 12: Ramachandran plot of LEA structural model predicted by PROCHECK

3.7. PPI network analysis of Mn-SOD.

Analysing the Mn-SOD protein with the STRING database, predicted that the functional partners of the protein was found as A0A0R0GD17, K7MML4_SOYBN, C6T0Z6_SOYBN, C6TFG9_SOYBN, C6TLX9_SOYBN, I1MNV0_SOYBN, A0A368UJ29, I1JUR5_SOYBN, I1LLT9_SOYBN and

I1MZU0_SOYBN with the respective confidence scores of 0.864, 0.864, 0.864, 0.864, 0.841, 0.840, 0.821, 0.821, 0.819 and 0.819. PPI network of Mn-SOD protein is shown in figure 13.

Statistical parameters of Mn-SOD PPI network such as number of nodes,

number of edges, average node degree average local clustering coefficient and PPI enrichment P-values were found to be 21, 125, 11.9, 0.818 and <1.0e-16. Table 7 depicts the PPI network analysis of Mn-SOD with predicted functional partners by Cytoscape V3.10.2.

Gene ontology (GO) analysis demonstrated that Mn-SOD protein and its functional partners participate, significantly in translation, mitochondrial translation and gene expression process, with these processes being highly significant and involving a substantial number of genes. The biological process enrichment of Mn-SOD for different metabolic activities is shown in figure-14

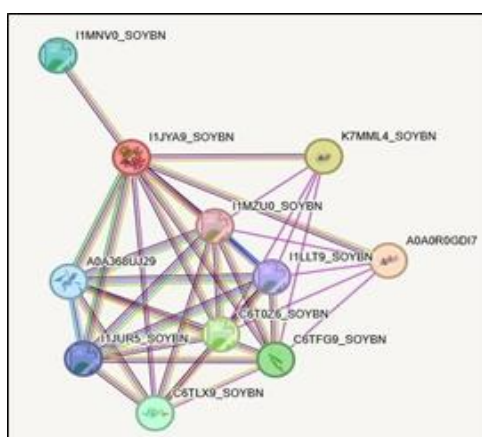


Fig 13: The PPI network of Mn-SOD and the predicted functional partners

Table 7: PPI network analysis of Mn-SOD and the predicted functional partners by Cytoscape v3.10.2

Protein	Betweenness Centrality	Closeness Centrality	Indegree	Outdegree	Neighbourhood Connectivity
A0A0R0GD17	0	0.692 30769 2	0	5	8.8
K7MML4_SOY BN	0.617 03703 7	1	6	4	6.6

C6T0Z6_SOYB N	0.102 22222 2	0.875	2	6	7.375
C6TFG9_SOY BN	0.102 22222 2	0.875	2	6	7.375
C6TLX9_SOY BN	0.105 92592 6	1	8	1	7.333333333
I1MNVO_SOY BN	0.105 92592 6	1	7	2	7.333333333
A0A368UJ29	0	0.818 18181 8	0	7	8.285714286
I1JUR5_SOYB N	0	0.714 28571 4	4	3	8.285714286
I1LLT9_SOYB N	0	0.75	3	4	8.285714286
I1MZU0_SOY BN	0	0	5	0	8.8

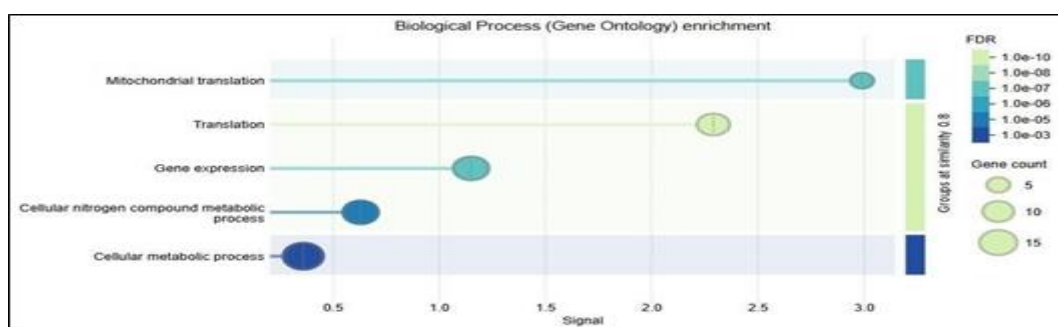


Fig 14: Biological process enrichment of Mn-SOD for different metabolic activities.

3.8. PPI network analysis of LEA

STRING database analysed and predicted that the functional partners of the protein was found as CEY00_Acc22222 (late embryogenesis abundant protein) CEY00_Acc29427 (Lipid II flippase), CEY00_Acc03466 (Low temperature induced protein), CEY00_Acc17823 (Late embryogenesis abundant protein), CEY00_Acc27820 (Protein EMB-1), CEY00_Acc26247 (4-hydroxy 4-methyl-2-oxoglutarate aldolase), CEY00_Acc27535 (4-hydroxy-4-methyl-2-oxoglutarate aldolase), CEY00_Acc22221 (late embryogenesis abundant protein), CEY00_Acc12568 (E3 ubiquitin protein) with the respective confidence scores of 0.628, 0.588, 0.581, 0.546, 0.505, 0.463, 0.454, 0.447, 0.447 and 0.422. PPI network of LEA proteins is shown in figure 15. Statistical parameters of LEA PPI network such as number of nodes number of edges, found to be 11, 15, 2.73, 0.783 and 0.0917. PPI network analysis of LEA with the predicted functional

partners by Cytoscape v3.10.2 is shown in table 8. This structure highlights the LEA proteins key role in biological processes related to stress tolerance and cellular protection, with potential co-regulation or co-operation among certain interacting partners. This aligns with the known biological functions of LEA proteins in plant stress responses.

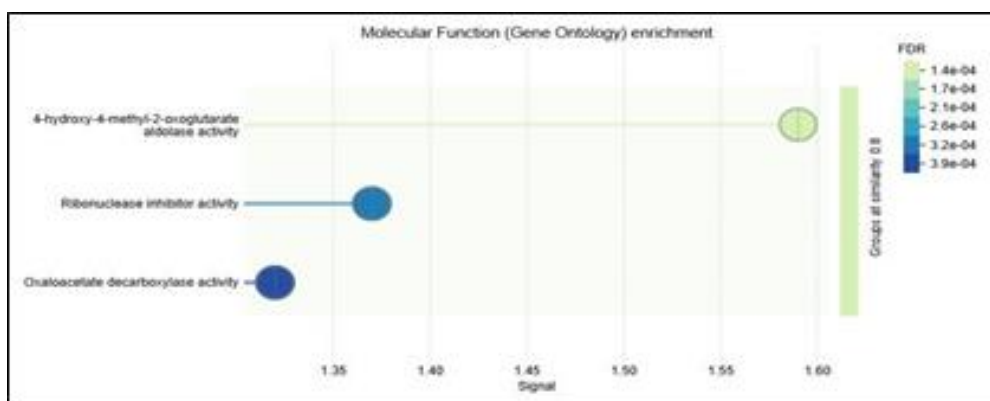
Gene ontology analysis reveals significant enrichment in aldolase activity, ribonuclease inhibition and oxaloacetate decarboxylase activity. This suggests that in addition to its established role in stress protection, LEA protein network may also be linked to diverse enzymatic and regulatory activities particularly those involved in metabolic processes and RNA protection. The most prominent activity is 4-hydroxy-4-methyl-2-oxoglutarate aldolase activity indicating a potential metabolic adaptation junction under Ni stress. Molecular junction enrichment of LEA for different metabolic activities is shown in figure 16



Fig 15: The PPI network of LEA and the predicted functional partners.

Table 8. PPI network analysis of LEA and the predicted functional partners by Cytoscape v3.10.2

Protein	Betweenness Centrality	Closeness Centrality	Indegree	Outdegree	Neighbourhood Connectivity
CEY00_Acc2 2222	0	1	0	2	7
CEY00_Acc2 9427	0	0	10	0	2
CEY00_Acc0 3466	0	1	3	1	4.5
CEY00_Acc1 7823	0	1	0	1	10
CEY00_Acc2 7820	0	1	0	3	5.666666667
CEY00_Acc2 6247	0	1	2	1	5.333333333
CEY00_Acc2 7535	0	1	0	1	10
CEY00_Acc2 2221	0	1	0	3	5.666666667
CEY00_Acc1 2568	0	1	0	1	10
CEY00_Acc2 4696	0	1	0	1	10

**Fig. 16.** Molecular function enrichment of LEA for different activities

The examination of PPI network yields substantial insights into molecular mechanisms that regulate plant stress responses. Proteins like Mn-SOD and LEA are recognised for their functions in alleviating oxidative and dehydrative stressors respectively. (38) asserted that Mn-SOD is a mitochondrial enzyme that facilitates the breakdown of superoxide radicals into hydrogen peroxide and oxygen; hence, the oxidative damage caused by environmental conditions such as drought, salinity and excessive radiation caused to the plants are safeguarded. PPI network of Mn-SOD revealed its function as an essential core protein, engaging with several antioxidative proteins, metabolic enzymes and regulatory factors (8). LEA proteins are produced during late embryogenesis and in response to abiotic stressors such as dehydration and salinity. They mainly serve as molecular chaperons safeguarding proteins and membranes from aggregation and denaturation induced by dehydration (4). PPI network evaluation of LEA proteins often reveal their interactions with diverse stress-responsive proteins including additional chaperons, enzymes related to metabolic adaptation and signalling proteins (34).

Mn-SOD and LEA proteins demonstrate centralization characteristics in protein-protein-interaction networks, signifying their essential role in stress response modules. Mn-SOD interacts with catalases, peroxidases and glutathione related enzymes, generating a formidable antioxidative system (26). (14) indicated that LEA proteins interact with metabolic enzymes and other protective proteins creating a module essential for cellular integrity during dehydration. PPI networks can facilitate the identification of innovative targets for genetic engineering or breeding initiatives focussed on enhancing agricultural stress tolerance (19).

CONCLUSION

The present study emphasises on Ni stress that induced significant alterations anatomically and proteomically in Ni tolerant chickpea cultivar, (*Cicer arietinum* L., ICCV 10102). Exposure to Ni has adversely effected root vascular system, leaf stomatal characteristics along with other impaired activities. Nevertheless, inoculation with PGPR MGNJ-01 effectively alleviated these anti effects by improving root and leaf anatomy. Proteomic analysis revealed the differential expression of Mn-SOD and LEA which are expressed as a response to stress. These proteins play a major role in anti-oxidative defense and cellular

protection. Under Ni and PGPR treatment, these proteins are involved in enhancing stress tolerance. This was further supported by *in silico* characterisation & protein-protein interaction in functional stability and regulatory importance of these proteins in stress adaptation mechanisms. On a whole, this study demonstrates that PGPR inoculation enhances Ni stress tolerance in chickpea by altering the anatomical features and activating protective molecular pathways. The potential application of PGPR suggests that it is a sustainable strategy for crop improvement in heavy metal contaminated soils.

REFERENCES

1. Ahmad P, Nabi G, Ashraf M. Metal tolerance in plants: Role of phytochelatins and metallothioneins. In: Abiotic Stress Responses in Plants. Springer; (2012). p. 199-212.
2. Alscher RG, Erturk N, Heath LS. Role of superoxide dismutases (SODs) in controlling oxidative stress in plants. *J Exp Bot.* (2002);53(372):1331-41.
3. Bansal H, Narang D, Jabalia N. Computational characterization of antifreeze proteins of *Typhula ishikariensis* – gray snow mould. *J Proteins Proteomics.* (2014);5(4):169-76.
4. Battaglia M, Olvera-Carrillo Y, Garcarrubio A, Campos F, Covarrubias AA. The enigmatic LEA proteins and other hydrophilins. *Plant Physiol.* (2008);148(1):6-24.
5. Buxbaum E. Fundamentals of protein structure and function. New York: Springer; (2007)
6. Czerwinska U, Calzone L, Barillot E, Zinovyev A. DeDaL: Cytoscape 3 app for producing and morphing data-driven and structure-driven network layouts. *BMC Syst Biol.* (2015);9(1):46
7. Franceschini A, Szklarczyk D, Frankild S, Kuhn M, Simonovic M, Roth A, et al. STRING v9.1: Protein-protein interaction networks, with increased coverage and integration. *Nucleic Acids Res.* (2013);41(D1):808-15
8. Gill SS, Tuteja N. Reactive oxygen species and antioxidant machinery in abiotic stress tolerance in crop plants. *Plant Physiol Biochem.* (2010);48(12):909-30.
9. Glick BR. Plant growth-promoting bacteria: mechanisms and applications. *Scientifica* (Cairo). (2012);2012:963401.
10. Glick, Bernard R. "Bacteria with ACC deaminase can promote plant growth and help to feed the world." *Microbiological research* 169.1 (2014): 30-39.

11. Gomathi R, Vasantha S, Shiyamala S, Rakkiyappan P. Differential accumulation of salt induced proteins in contrasting sugarcane genotypes. *EJBS*. (2013);6(1):7-11
12. Guruprasad K, Reddy BVP, Pandit MW. Correlation between stability of a protein and its dipeptide composition: a novel approach for predicting in vivo stability of a protein from its primary sequence. *Protein Eng*. (1990);4:155-64
13. Gusain YS, Singh US, Sharma AK. Plant growth-promoting rhizobacteria: Potential candidates for Ni phytoremediation. *Ecotoxicol Environ Saf*. (2015);117:126-37.
14. Hundertmark, Michaela, and Dirk K. Hinch. "LEA (late embryogenesis abundant) proteins and their encoding genes in *Arabidopsis thaliana*." *BMC genomics* 9.1 (2008): 118
15. Ikai A. Thermostability and aliphatic index of globular proteins. *J Biochem*. (1980);88:1895-ISS Insights. Ni
16. Johansen DA. Plant microtechnique. (1940): xi-523
17. Kaushal M, Wani SP. Plant-growth-promoting rhizobacteria: Drought stress alleviators to ameliorate crop production in drylands. *Ann Microbiol*. (2016);66:35-42.
18. Kelley LA, Mezulis S, Yates CM, Wass MN, Sternberg MJ. The Phyre2 web portal for protein modeling, prediction and analysis. *Nat Protoc*. (2015);10(6):845-58
19. Kosova K, Vitámvás P, Prášil IT, Renaut J. Plant proteome changes under abiotic stress—contribution of proteomics studies to understanding plant stress response. *J Proteomics*. (2014);74(8):1301-32
20. Kottapalli KR, Payton P, Rakwal R, Agrawal GK, Shibato J, Burow M, et al. Proteomics analysis of mature seed of four peanut cultivars using two-dimensional gel electrophoresis reveals distinct differential expression of storage, anti-nutritional, and allergenic proteins. *Plant Sci*. (2008);175(3):321-9.
21. Kraus IE, Arduin M. Manual básico de métodos em morfologia vegetal. Seropedica: Editora da Universidade Rural; (1997).
22. Krishnasamy L, Masilamani Selvam M, Jayanthi K. Novel in silico approach of anticancer activity by inhibiting Hemopexin proteins with *Indigofera aspalathoides* plant constituents at active site. *Asian J Pharm Clin Res*. (2015);8(3):159-64.
23. Kumar A, Singh S, Gaurav AK, Srivastava S, Verma JP. Plant growth-promoting bacteria: Biological tools for the mitigation of salinity stress in plants. *Front Microbiol*. (2017);8:1766
24. Kyte J, Doolittle RF. A simple method for displaying the hydropathic character of a protein. *J Mol Biol*. (1982);157:105-32.
25. Ma Y, Oliveira RS, Freitas H, Zhang C. Biochemical and molecular mechanisms of plant–microbe–metal interactions: relevance for phytoremediation. *Front Plant Sci*. (2016);7:918.
26. Mittler R, Vanderauwera S, Gollery M, Van Breusegem F. Reactive oxygen gene network of plants. *Trends Plant Sci*. (2004);9(10):490-8.
27. Neelamathi E, Vasumathi E, Bagyalakshmi S, Kannan R. In silico prediction of structure and functional aspects of a hypothetical protein of *Neurospora crassa*. *J Cell Tissue Res*. (2009);9:1889-94.
28. Rajkumar M, Ae N, Prasad MNV, Freitas H. Potential of siderophore-producing bacteria for improving heavy metal phytoextraction. *Trends Biotechnol*. (2010);28(3):142-9
29. Nisarga P, Ramdas Bhat, Sinchana S Bhat. Pharmacogenomics in Pediatric Cancer Patients Treated with Irinotecan: A Systematic Review. *Oral Sphere Journal of Dental and Health Sciences*. 2025;1(4):244-258.
30. Seregin I, Kozhevnikova AD. Physiological role of nickel and its toxic effects on higher plants. *Russ J Plant Physiol*. (2006);53(2):257–277.
31. Sharma P, Dubey RS. Lead toxicity in plants. *Braz J Plant Physiol*. (2005);17(1):35-52.
32. Singh A, Prasad SM, Singh S. Differential response of superoxide dismutase isoenzymes in chickpea under nickel stress. *Environ Sci Pollut Res*. (2016);23(7):6681-91
33. Singh S, Parihar P, Singh R, Singh VP, Prasad SM. Heavy metal tolerance in plants: role of transcriptomics, proteomics, metabolomics, and ionomics. *Front Plant Sci*. (2015);6:1143
34. Tunnacliffe A, Wise MJ. The continuing conundrum of the LEA proteins. *Naturwissenschaften*. (2007);94(10):791-812.
35. Ulmschneider MB, Sansom MSP. Amino acid distributions in integral membrane protein structures. *Biochim Biophys Acta Biomembr*. (2001);1512:1-14
36. Vessey JK. Plant growth promoting rhizobacteria as biofertilizers. *Plant Soil*. (2003);255(2):571-86
37. Vidhya VG, Upgade A, Bhaskar A, Dipanjana D. In silico characterization of Bovine (*Bos taurus*) antiapoptotic proteins. *J Proteins Proteomics*. (2012);3(3):187-96.
38. Wang W, Vinocur B, Altman A. Plant responses to drought, salinity and extreme temperatures: towards genetic engineering for stress tolerance. *Planta*. (2016);218(1):1-14.
39. Yadav SK. Heavy metals toxicity in plants: an overview on the role of glutathione and phytochelatin in heavy metal stress tolerance of plants. *S Afr J Bot*. (2010);76(2):167-79
40. Yusuf M, Fariduddin Q, Ahmad A. Nickel: An overview of uptake, essentiality, toxicity and tolerance in plants. *Bull Environ Contam Toxicol*. (2011);86(1):1-17
41. Zaccaria D, Greco R, MacWilliams H, Bozzaro S, Ceccarelli A. UGUS, a reporter for use with destabilizing N-termini. *Nucleic Acids Res*. (1998);26:1128-9